

Experimental Results with a Very-Heavy-Ion  
RFQ Accelerating Structure at GSI

R.W. Müller, U. Kopf, J. Bolle, S. Arai\*, P. Spädtke  
GSI Darmstadt, Fed. Rep. of Germany  
\*INS Tokyo, Japan

1. Introduction and Summary

Radio frequency quadrupole (RFQ) focusing and accelerating devices are a novel technology preparing a link between static injectors and magnetically focused linacs for ions. They solve the problem of reliable, well-controlled and well-focused acceleration of intense beams of light ( $H^+$ ) or heavy ( $Xe^+$  to  $U^+$ ) ions. Though an old idea, Kapchinskij<sup>1</sup> first developed a strategy of designing an RFQ linac.

We attacked the problem of accelerating very heavy ions up to  $A/q \leq 130$ , or even more depending on the choice of frequency. Ion beams like this will be used to increase the brilliance of present heavy ion linacs by a factor  $10^3$  to  $10^4$ , and ultimately to construct linacs for heavy-ion driven, inertially confined thermonuclear fusion. This work has been supported by the Federal Ministry of Research and Technology of FRG within the heavy-ion inertial confinement (SIT) program.

For a given normalized beam acceptance, the frequency has to be chosen  $\propto (q/A)^{1/2}$ ; for  $\alpha_t^N = 0.5 \text{ mm} \cdot \text{mrad} = 5 \cdot 10^{-7} \text{ m}$ ,  $A/q \approx 130$ , the frequency is around 13.5 MHz. The design beam current is 0.2 to 0.4 mA  $\cdot (A/q)$ . A frequency as low as this dictates the search for new RF cavity techniques since the  $H_{210\text{circ}}$ -like cavity mode used so far for light ions, is no more applicable for several reasons. We have found a good solution with the split-coaxial cavity type, and with Q electrodes of cylindrical shapes suspended in rings, a solution which presents very much technical comfort.

The first module (of five for one complete tank) is in operation with a beam since November 1983. It takes the input energy of 2.3 keV/amu to an output energy of 4.3 keV/amu, and acts as a vigorous buncher containing a radial matcher, a shaper and the first part of a gentle buncher section. The results are very satisfactory. The next four modules are under fabrication. The 80 kW r.f. amplifier still is provisional and will be replaced by a 1 MW amplifier (pulse power).

2. Description

The RF resonator is of the split-coaxial T(E)M type<sup>2</sup> which can be described as a TEM transmission line with suppressed E field, since the sum of product of the voltages on the parts of the split inner conductor times the partial capacities towards the outer conductor, is zero everywhere. This provides a perfect voltage flatness along the RFQ channel and a homogeneous current distribution on the inner conductor. Fig. 1 shows the voltages along the split inner conductor parts as a mental

Table I: COMPARISON OF DESIGN PARAMETERS

|  | Profile A  |                                | Profile B   |
|--|--|--------------------------------|---|
|  | (proton model)   |                                |   |
| RF frequency                               | 13.55 MHz  | 54.2 MHz                       | 13.55 MHz   |
| Free aperture radius, R                    | 12 mm  | 3 mm                           | 6 mm  |
| Normal acceptances,                        |  |                                |   |
| transv., $\alpha_t^N$                      | $1 \cdot 10^{-6} \text{ m}$  | $0.25 \cdot 10^{-6} \text{ m}$ | $0.5 \cdot 10^{-6} \text{ m}$                     |
| long., $\alpha_l^N$                        | $7.2 \cdot 10^{-6} \text{ m}$  | $1.8 \cdot 10^{-6} \text{ m}$  | $5.5 \cdot 10^{-6} \text{ m}$                     |
| Phase adv. per $\beta\lambda$ cell,        |  |                                |   |
| transv., $\sigma_{to}$                     | 0.27...0.45...0.4  |                                | 1.4...0.8   |
| long., $\sigma_{lo}$                       | 0.77...0.25...0.13   |                                | 0.73...0.18                                       |
| Injection: $\beta_1^0, A_1^0, T_1$         | 0.227%; 2.4 keV/amu  |                                | 0.220%; 2.26 keV/amu                              |
| Nom. RF volt. ampl., $\frac{q}{A} U_{RF}$  | 1.9 kV/amu   |                                | 1.22 kV/amu                                       |
| Av. accel. gradient, $\frac{q}{A} E_{eff}$ | 6.7 $\frac{\text{kV}}{\text{m} \cdot \text{amu}}$ 26.9 $\frac{\text{kV}}{\text{m} \cdot \text{amu}}$ |                                | 5.0 $\frac{\text{kV}}{\text{m} \cdot \text{amu}}$ |
| RMS? Length                                | Yes, but imperfect; 28 $\lambda$   |                                | Yes; 28 $\lambda$                                 |
| Shaper? Length                             | No; -  |                                | Yes; 19 $\lambda$                                 |
| Gentle buncher length                      | ~100 $\lambda$   |                                | 112 $\lambda$                                     |
| Transv. current limit,                     |  |                                |   |
| 40% tune depr., $\frac{q}{A} I_{lim}$      | 0.13 mA/amu  |                                | 0.2 mA/amu  |
| 60% tune depr., $\frac{q}{A} I_{lim}$      | (?) 0.26 mA/amu  |                                | 0.4 mA/amu  |

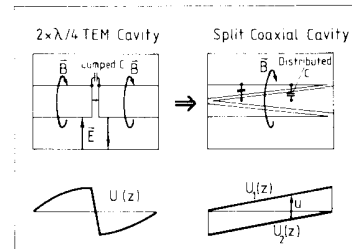


Fig. 1: Mental evolution of a  $2 \times \lambda/4$  TEM cavity into an SC cavity.

evolution of a  $2 \times \lambda/4$  push-pull TEM cavity. The general features are

- a very stable r.f. mode with inherent voltage flatness;
- modularity, i.e. a large number of cavities can be coupled providing a continuous bed for RFQ electrodes;
- good shunt impedance, good mechanical stability, easy cooling and easy adjustment.

The split coaxial (SC) cavity can be equipped either with continuous RFQ vanes, or with individual pieces of cylindrical RFQ electrodes, each  $\beta\lambda$  long or a little shorter, suspended by rings every  $\beta\lambda/2$ . The latter solution, which has been adopted, provides a reliable suppression of dipole fields, helps shaping a higher axis potential amplitude  $A_1$  where needed, and provides a high mechanical stability and a good definition of the aperture radius R, but also contributes to a higher distributed capacity  $C'$ . This latter effect gradually vanishes from the second module on. The ring stems serve

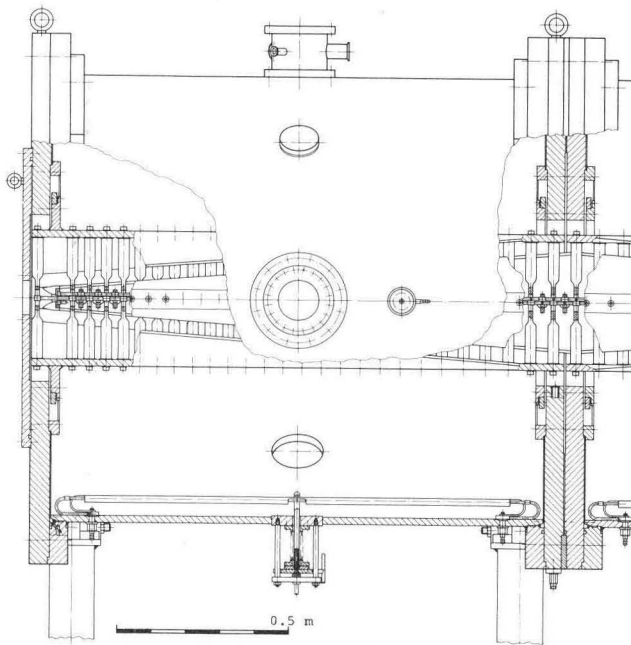


Fig. 2: Long section of the structure

to conduct r.f. and beam loss heat from the RFQ electrodes to the water-cooled inner conductor pieces of the r.f. cavity. Though requiring some milling, this solution turned out to be good and cheap; the production cost of a unit shown in fig. 3 is about 500 DM, and 53 of these units are in module 1. The material for them as well as for the RFQ electrodes is Elmedur X, copper containing 0.75 % of Cr, which is comfortable to machine. No brazing, welding or soldering is used in the high-field region. The other parts of the cavity, seen in fig. 2 in the longitudinal section, are made from mild steel, 100  $\mu\text{m}$  Cu-plated. Fig. 4 shows the cavity during assembly.

### 3. Quadrupole Profile and Beam Dynamics

A constant-aperture profile has been chosen, aperture radius = R, except for the shaper section where the aperture is widened a little to keep  $\sigma_{to}$  below  $\pi/2$ .

Neither  $\sigma_{to}$  nor  $\sigma_{lo}$  (see fig. 5) are constant along the gentle buncher section; the bunch length  $l_{\text{bunch}}$  is increasing. Care has been taken, however, to keep the longitudinal bucket acceptance constant or with a slight overshoot, and to keep  $\sigma_{to} \cdot l_{\text{bunch}}$  constant to provide a constant transverse space charge limit.

The dynamic parameters: accelerating potential amplitude  $A_1$ , gradient weakening function  $1-B_0 \equiv X$ , and higher harmonics as  $A_3$  and  $B_2$ , have been computed numerically by a computer code ELTROC which simulates an electrolytic trough. The velocity profile has been generated sectionwise with a parametric interpolation giving a quick survey of properties, lengths etc; this procedure will not be described here in detail. The

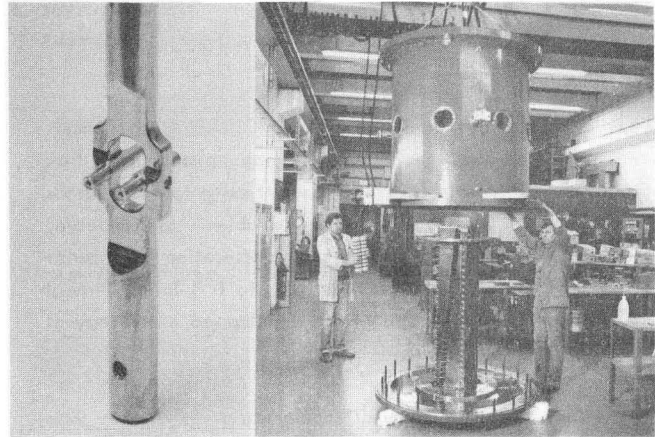


Fig. 3: Electrode & Stem Unit

Fig. 4: Assembly

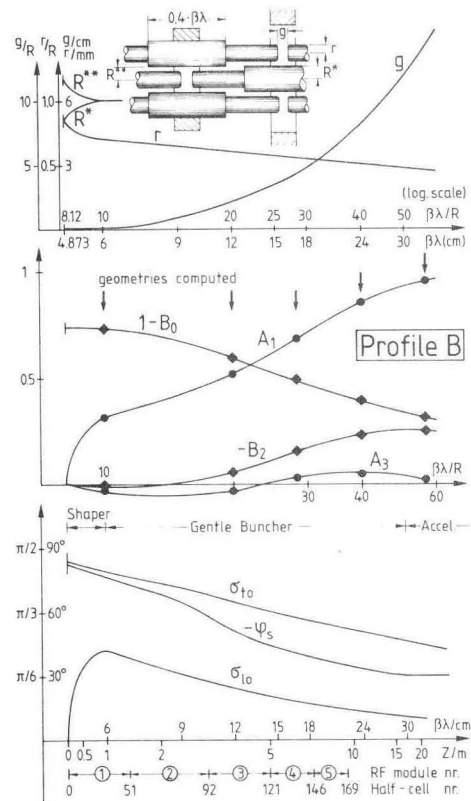


Fig. 5: Focusing and accelerating profile

results are given in fig. 5 and table I, named "profile B".

The transverse phase advance  $\sigma_{to}$  has been chosen as high as possible, but below  $\pi/2$ , to provide optimal beam stability. In this respect profile B is improved over profile A (table I) which had been applied in the Frankfurt proton model<sup>2</sup>; this latter profile reaches its best experimental performance at voltages which are somewhat higher than the design voltage.

The radial-matching section (RMS),  $2\beta\lambda$  long, is of a special design since, at the cavity entrance, one pair of



electrodes is at ground potential. Therefore, the RMS has to provide not only a linear ramp of the gradient, but also of the axis potential. Its design is seen from fig. 2.

A similar RMS,  $1 \beta\lambda$  long, is attached at the beam output. The necessity of such a "matching-out" section has been encountered during the beam experiments; this device, consisting of copper electrodes fixed on the last cylindrical RFQ, had a big improving effect on beam quality.

#### 4. Voltage Tests

Application of r.f. voltages began in March, 1983. After an initial improvement of the design of the screws connecting the electrode stems to the split conductors, and after conditioning, r.f. voltages (peak) of 120 kV have been reached with no sparking, and 140 kV with much sparking. 155 kV is sufficient to accelerate particles of  $A/q$  of 130.

#### 5. Beam Tests

So far beam tests have been done with an  $^{40}\text{Ar}^+$  and a  $^{82-86}\text{Kr}^+$  beam; at these levels (40 kV or 85 kV resp.) there is no sparking, no X-rays, and no r.f. power and beam power problems.

The source in use is ELSIRE<sup>4</sup>. There is a triode extraction gap, followed by an acceleration gap and a magnetic quadrupole quadruplet. Negative potential barriers are used to prevent space-charge compensating electrons from escaping into the acceleration gaps.

The beam current record with  $\text{Ar}^+$  has been 6 mA (pulsed) in the final cup, the standard current is 3 mA; with  $\text{Kr}^+$ , 8 mA was the maximum so far.

A beam of this strength causes a big beam-load effect in the cavity (fig. 6) if it is not compensated by so-called feed-forward in the amplifier chain (so far it is not used). Since the cavity needs time (about the r.f. build-up time) to accommodate to the conditions with beam, the first 400  $\mu\text{s}$  of the beam pulse (fig. 7, from a fast 50 Ohms cup) are not nice, and useless for high-standard applications. The problem of the next future will be to produce a "beautiful" beam pulse.

After these 400  $\mu\text{s}$  of transients, the beam micropulses are of high quality and look as predicted (fig. 8, for  $\text{Ar}^+$ ) The clean "valley bottoms" between pulses containing no idle beam parts, were the result of some improvement of the injection system, especially of good matching. Before this improvement, the valleys contained some beam, probably  $\text{Ar}^{++}$ .

#### References

1. I.M. Kapchinskij, V.A. Tepljakov, Prib. Techn. Eksp. 2 (1970), 19
2. R.W. Müller, Layout of a High-Intensity Linac for Very Heavy Ions with RFQ Focusing. GSI-Rep. 79-7.
3. J. Müller, Untersuchungen an HF-Quadrupol-Beschleuniger-Strukturen. Thesis, Univ. of Frankfurt/M., 1983
4. R. Keller, GSI Sci. Rep. 1979, GSI 80-3, 212. Photographs by A. Zschau, GSI.

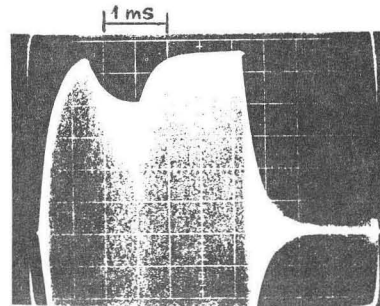


Fig. 6  
RF voltage signal with beam pulse loading

Fig. 7 Fig. 8  
Beam pulse shapes  
(x 25 Ohm)

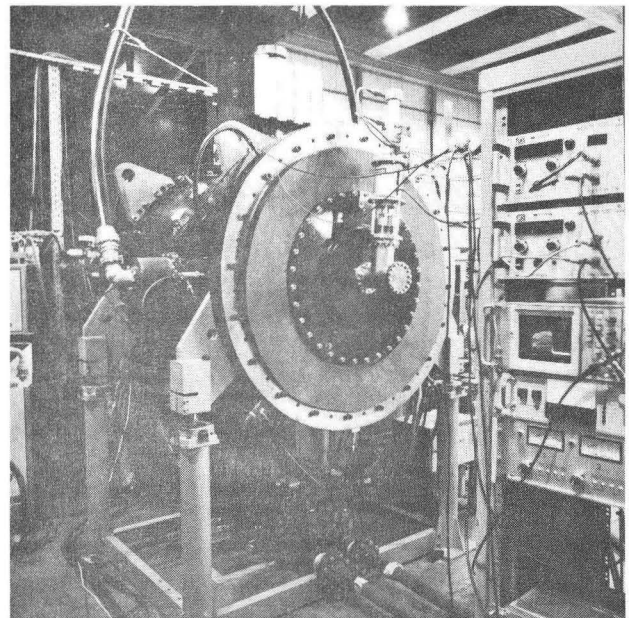
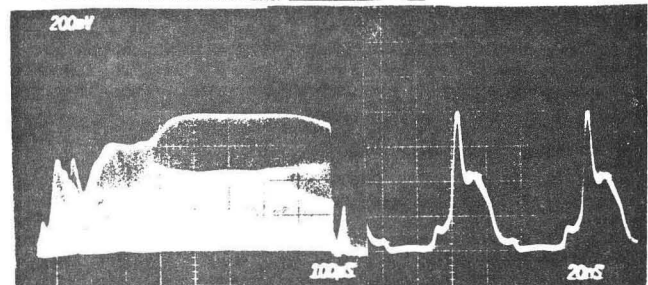


Fig. 9: RFQ Module 1 during beam test. At the output a 50 Ohms cup catches the beam and displays it on the scope screen in the foreground. Around the output flange, a wooden shield protects the copper surface which is to give an r.f. contact to module no. 2 which does not yet exist. An r.f. cable feeds r.f. power from an 80 kW amplifier in the background.